Supplemental Materials for: Ginsenoside Rg3, a gating modifier of EAG family K^+ channels

Wei Wu, Alison Gardner, Frank B. Sachse and Michael C. Sanguinetti

Molecular Pharmacology

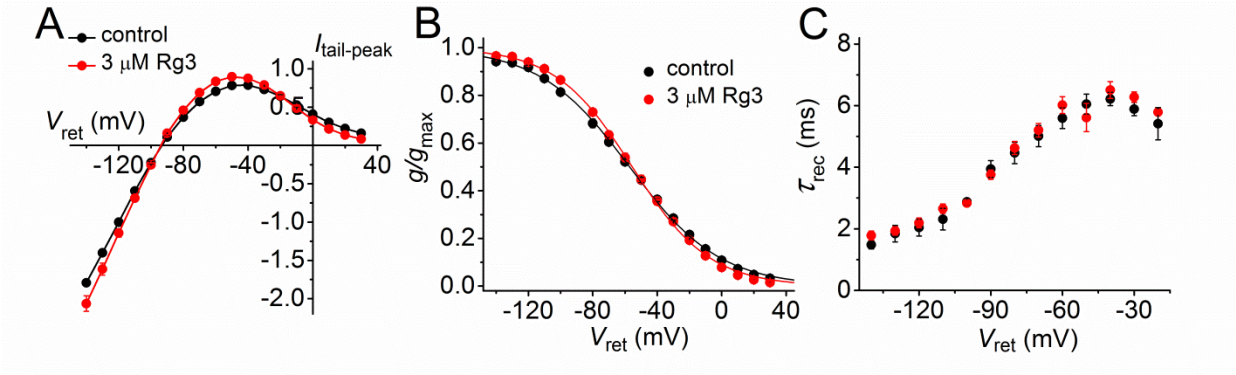

Supplemental Figure 1. Inactivation of hERG1 channels is not altered by Rg3. (A) Fully-activated $I_{tail-peak}$-V_{ret} relationships in the absence and presence of 3 μM Rg3. Data were normalized relative to $I_{tail-peak}$ at –120 mV under control conditions (2-way ANOVA, $p < 0.01$). (B) Rg3 does not affect voltage-dependence of hERG1 inactivation. Data were fitted with a Boltzmann function (smooth curve). For control, $V_{0.5}$ = –57.2 ± 1.2 mV; k = 27.7 ± 0.6. For 3 μM Rg3, $V_{0.5}$ = –56.1 ± 1.3 mV; k = 24.9 ± 0.2 (paired t-test, p = 0.2). (C) Effect of Rg3 on τ_{rec}, the time constant for recovery from hERG1 channel current inactivation (2-way ANOVA, p = 0.04). For all panels, n = 5.

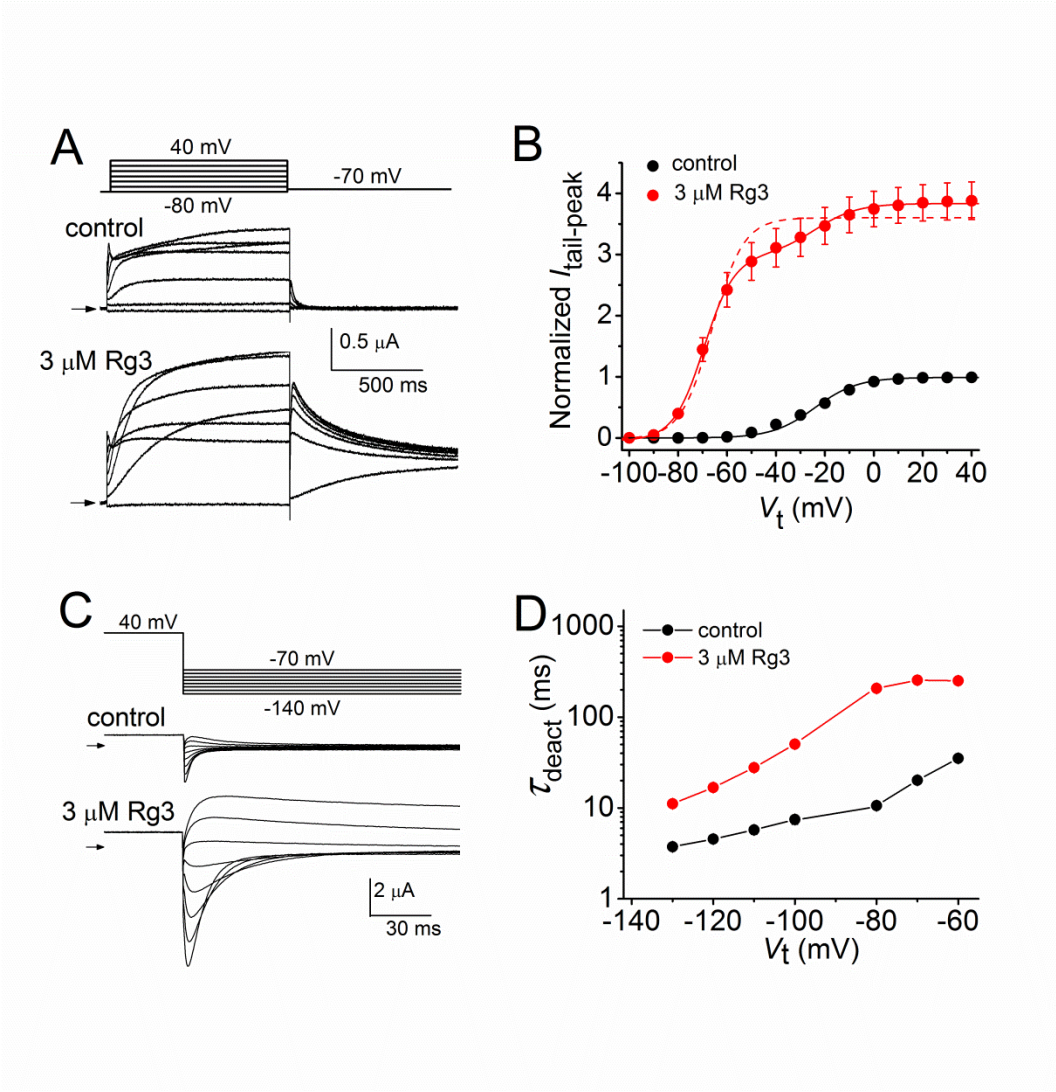

Supplemental Figure 2. Concentration and voltage dependent effects of Rg3 on N-deleted and C-truncated hERG1 channel currents. (A) Representative currents recorded from a single oocyte before (control) and after treatment with 3 μM Rg3. Upper panel shows voltage pulse protocol. (B) Effects of 3 μM Rg3 on voltage dependence of N/C-del hERG1 channel activation using 1 s test pulses. $I_{tail-peak}$ in the presence of Rg3 was normalized relative to the maximum $I_{tail-peak}$ measured under control condition (n = 11). Control data were fitted with a single Boltzmann function ($V_{0.5}$ = –25.5 ± 1.6 mV, k = 10.3 ± 0.2). Rg3 data were poorly fit using a single Boltzmann function (dashed smooth curve). *G-V* relationships measured after application of Rg3 were fitted with the sum of two Boltzmann functions, with component "1" assumed to represent unbound channels having $V_{0.5}$ and k fixed at control values and component "2" assumed to represent the Rg3-bound fraction of channels. For 3 μM Rg3: A_{max1} = 0.25, A_{max2} = 0.75, $V_{0.5(2)}$ = –69.1 ± 0.6 mV, k_2 = 6.1 ± 0.2. (C) Representative tail currents recorded in an oocyte under control conditions and after treatment with 3 μM Rg3. Upper panel shows voltage pulse protocol. (D) Effect of 3 μM Rg3 on the time constants for current deactivation (τ_{deact}) (n = 7; 2-way ANOVA, p < 0.0001).

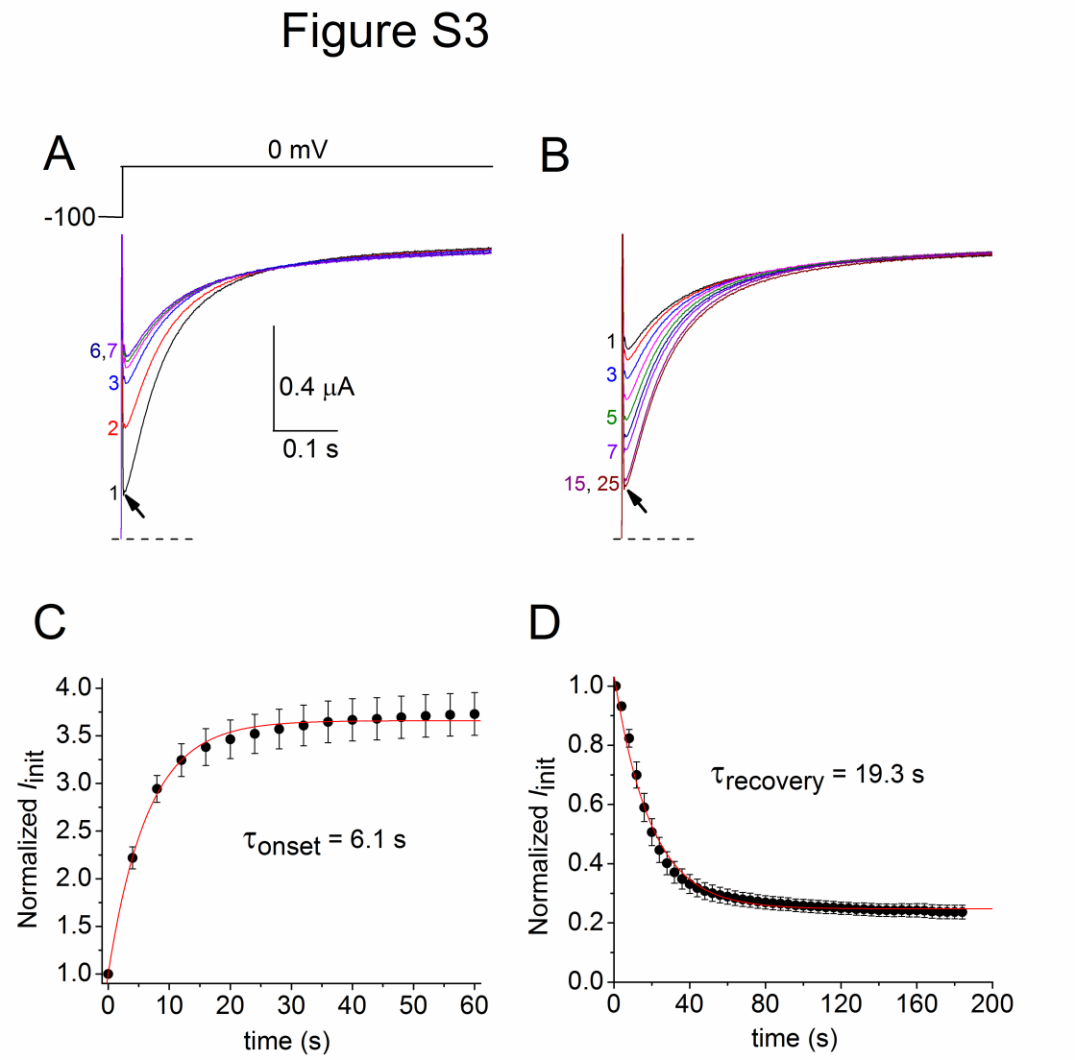

Supplemental Figure 3. Onset of and recovery from effects of Rg3 on hELK1 channels. (A) Onset of 0.3 µM Rg3 effects on hELK1 channel currents measured during repetitive pulsing to 0 mV from a holding potential of −100 mV. Pulses (0.6 s duration) were applied once every 4 s. After applying 10 pulses under control conditions, the bath solution was rapidly switched to a solution containing Rg3. Plot shows individual current traces recorded in response to the 10th control pulse (labeled "1") and subsequent pulsing after solution switching (labeled "2", etc). All 10 control currents were superimposable (not shown). The initial outward current (I_{init}, indicated by arrow) was measured immediately after the outward capacitance current transient. (B) Current traces recorded in the presence of 0.3 µM Rg3 (labeled "1") and subsequent pulses after initiation of solution washout (labeled "2..3..7, etc"). In panels B and C, dotted line represents zero current level. (C) Currents were normalized to I_{init} under control conditions and plotted as a function of time after switching chamber perfusate from control solution to 0.3 µM Rg3 solution. The data were fitted with a single exponential function to estimate the time constant for onset of Rg3 action (τ_{onset} = 6.1 ± 0.8 s, n = 10). (D) Kinetics of recovery of I_{init} during rapid washout of 0.3 µM Rg3 solution ($\tau_{recovery}$ = 19.3 ± 1.8 s, n = 10). Currents were normalized to I_{init} measured in the presence of Rg3.

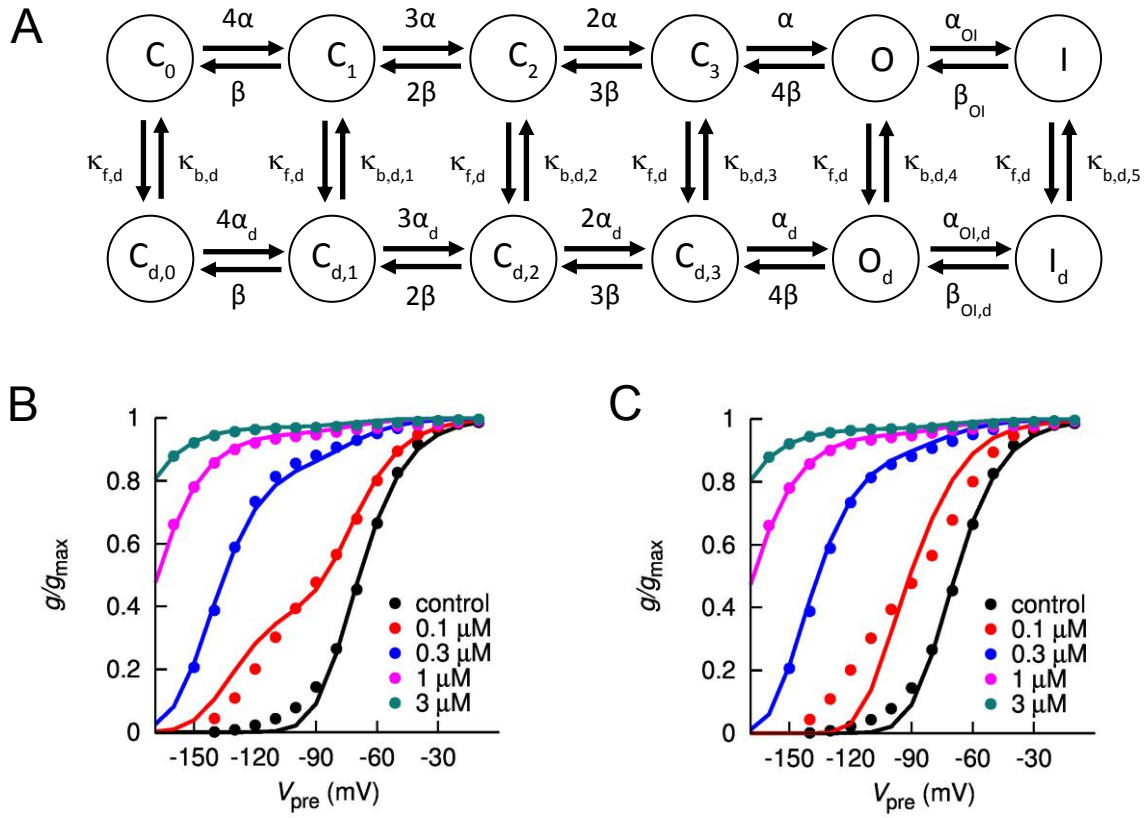

Supplemental Figure 4. Comparison of simulated G-V relationships for hELK1 activation. (A) Schematic of two-compartment Markov model. The two compartments, $C_0 \ldots I$ and $C_{d,0} \ldots I_d$, represent channels in the absence of Rg3 and populations of channels in the presence of Rg3. Note that $\kappa_{f,d} = \kappa_{f0,d}[Rg3]$. *G-V* relationships were simulated with rate coefficients $\kappa_{f,d}, \kappa_{b,d}, \kappa_{b,d,1}, \ldots, \kappa_{b,d,5}$ decreased to 1% (B) or increased 100 times (C).

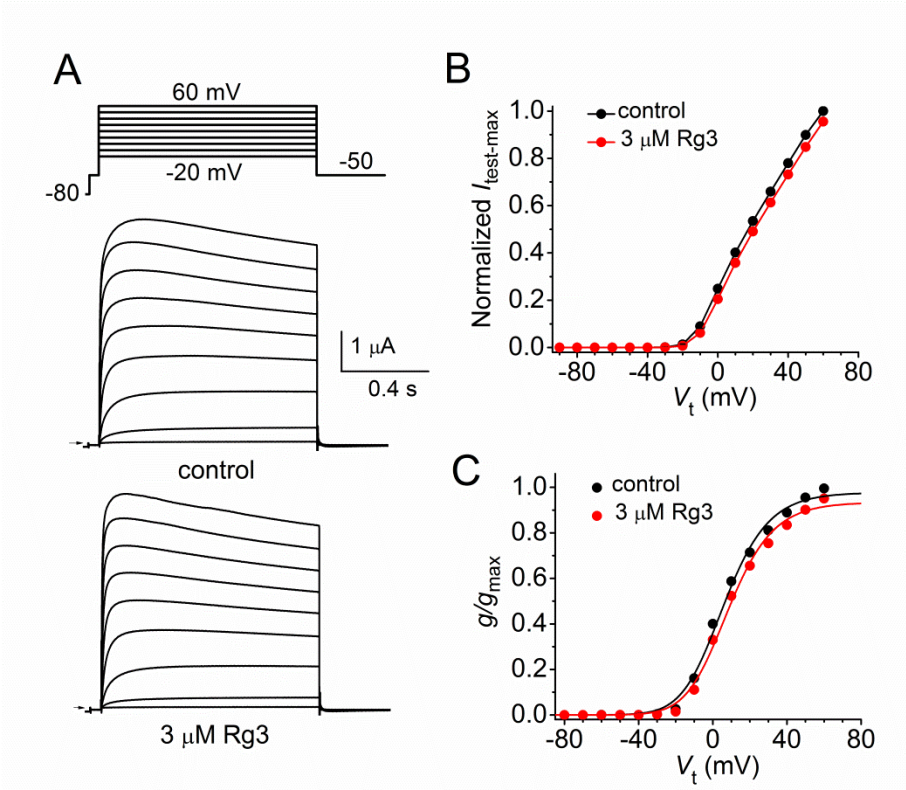

Supplemental Figure 5. Rg3 does not alter gating of Kv1.5 channels. (A) Representative Kv1.5 channel currents recorded in a single oocyte under control conditions and after treatment with 3 μM Rg3. Upper panel show voltage pulse protocol used to elicit currents. (B) $I_{test-max}$-V_t relationships measured in the absence and presence of 3 μM Rg3. Currents were normalized to the control current at +60 mV (n = 10). (C) Voltage dependence of Kv1.5 channel activation (n = 10). Data were fitted with a Boltzmann function to the 2nd power (smooth curves). For control, $V_{0.5}$ = −6.0 ± 0.9 mV and k = 13.8 ± 1.0. For Rg3, $V_{0.5}$ = −4.0 ± 0.9 mV and k = 13.9 ± 1.0. In panels B and C, SEM bars are smaller than symbol size.

Feature	Weighting Factor	Control
$I_{test\text{-}max}$	4	0.396
$\tau_{test\text{-}s}$	1	0.144
$\tau_{inact\text{-}s}$	1	0.229
A_{deact}	2	0.483
$\tau_{deact\text{-}s}$	1	0.292
$\tau_{deact\text{-}s}$	1	0.140
$1\text{-}I_{inact\text{-}max}$	2	0.235
$g_{test}/g_{test\text{-}max}$	4	0.301
$1\text{-}g_{test,\text{-}10mV}$	0.5	0.105
$C_0+C_1+C_2+C_3$	20	0.249
O+I	1	0.000

Table S1: Features for model fitting and their fit errors $E_i = \|f_{m,i} - f_{e,i}\|_2 / \|f_{e,i}\|_2$. Weighting factors were applied to emphasize or deemphasize features.

States	Symbol	Value
0^{th} closed state	C_0	1
1^{st} – 3^{rd} closed state	C_1, …, C_3	0
Open state	O	0
Inactivated state	I	0

Table S2: Initial values for model.

Parameter	Symbol	Control	Unit
C-C and C-O transitions	α_0	43.847	s^{-1}
	z_α	0.559	
	β_0	0.025	s^{-1}
	z_β	1.157	
O-I transitions	α_{OI}	1.167	s^{-1}
	$z_{\alpha OI}$	-0.235	
	β_{OI}	5.504	s^{-1}
	$z_{\beta OI}$	0.220	

Table S3: Rate constant parameters for model.

[Rg3]	Scaling $\alpha_{0,d}$	[Rg3] $\kappa_{f0,d}$
0 µM	$10^{0.1}$	0
0.1 µM	$10^{1.8}$	0.0043
0.3 µM	$10^{2.2}$	0.0167
1 µM	$10^{3.1}$	0.0256
3 µM	$10^{3.7}$	0.0300

Table S4: Scaling factors for $\alpha_{0,d}$ and [Rg3]$\kappa_{f0,d}$ of two-compartment model.